PHYSICAL REVIEW A VOLUME 22, NUMBER 6 DECEMBER 1980

D^- production by charge transfer of 0.3–10-keV D^+, D^0, and D^- in cesium-, rubidium-, and sodium-vapor targets

A. S. Schlachter, K. R. Stalder, and J. W. Stearns
Lawrence Berkeley Laboratory, University of California, Berkeley, California 94720
(Received 21 April 1980)

Equilibrium charge-state fractions for 0.3–10-keV D ions and atoms in cesium-, rubidium-, and sodium-vapor targets are reported. The D^- yield from charge transfer in a thick cesium-vapor target exceeds 30 percent at energies below 800 eV. The high D^- yield in cesium vapor is consistent with recent calculations of the cross sections σ_{0-} and σ_{-0} at low energies; at energies above 2.5 keV, the D^- yield is consistent with our measurements of σ_{0-} and σ_{-0}. The D^- yield from charge transfer in rubidium vapor is similar to that for cesium vapor. For sodium vapor, however, there is a broad maximum of about 10 percent D^- yield at about 3 keV, with slight structure at lower energies, implying structure in one of the charge-transfer cross sections.

I. INTRODUCTION

Electron capture and loss between a fast projectile and a target atom or molecule has been extensively studied and is fairly well understood both experimentally and theoretically for a wide range of systems. Systems involving energetic hydrogen beams interacting with alkali-metal vapors have, however, not yielded consistent results between the various experiments reported in the literature, and theoretical models have done very little to resolve these discrepancies.

Many studies are now underway to find methods for producing intense, high-energy, negative hydrogen beams (particularly D^- beams) for use in heating large fusion plasmas (via neutralized D^- beams).[1,2] Some of these studies involve the process of muliple charge transfer of relatively low-energy deuterium beams in metal-vapor targets to produce D^- ions which are subsequently accelerated and neutralized to produce high-energy neutral beams.

We have measured the equilibrium fractions F_+^∞, F_0^∞, and F_-^∞ of the total fast deuterium beam which emerges from vapor targets of sodium, rubidium, and cesium. The incident beams were D^+, D^0, and D^- in the energy range 300 eV to 10 keV. We measured the cross sections σ_{0-} and σ_{-0} in cesium vapor in the energy range 2.5–10 keV. We have also made a few measurements for D_2^+ and D_3^+ incident on cesium and sodium vapors.

Negative-ion sources are generally of two types. The simplest is direct extraction from a plasma where the ions may be produced in the plasma itself or on a metallic (often cesium-coated) surface.[3–6] A principal drawback of this method is that it is necessary to suppress electrons while extracting the negative ions. This type of source is often used in cyclotrons, for example, where the magnetic field separates the electrons from the negative-ion beam so they can be skimmed off before they consume much power.

The other type of negative-ion source extracts positive ions from the plasma at low energy; these ions are converted to negative ions by a subsequent collision in a gas or metal-vapor target[7–11] before being further accelerated. The disadvantage of this type of source is the lowered intensity due to space-charge effects, scattering, or small electron-capture cross sections at energies high enough to overcome the first two effects. This type of source is often employed in tandem accelerators. A similar method is also employed in certain polarized D^- sources.[12]

The earliest report of a large D^- yield by charge transfer in a metal vapor was by Drake and Krotkov,[13] who remarked in 1966 that as much as 25 percent of 1-keV D^+ could be converted to D^- in a thick cesium-vapor target. D^- formation in metal vapors has been extensively studied since then.[14] These measurements in cesium vapor are summarized in Table I.[14–30] One earlier experiment[23] and preliminary results from the present experiment[14,26] are the only F_i^∞ measurements previously reported for D or H in rubidium vapor. Previous results for sodium-vapor targets are summarized in Table II.[16,17,26–28,30–34] Calculated as well as measured cross sections, σ_{0-} and σ_{-0}, for hydrogen and deuterium in cesium vapor have previously been reported by several authors.[18,21,24,26,35–41]

The cross section for a particle in charge state j which changes to charge state k in a single collision is represented by σ_{jk}. For deuterium colliding with a target X, σ_{0-} describes the process

$$D^0(1s)+X \rightarrow D^-+\cdots \qquad (\sigma_{0-}), \qquad (1)$$

and σ_{-0} describes the process

$$D^-+X \rightarrow D^0(nl)+\cdots \qquad (\sigma_{-0}). \qquad (2)$$

The fraction of the total beam leaving the tar-

TABLE I. Summary of measurements of equilibrium yields and optimum conversion efficiencies for deuterium ions and atoms in cesium vapor.

Author	Reference	Measured	D energy range (keV)
Bohlen *et al.* (1968)	15	η_-^{opt}	1–4
Grüebler *et al.* (1969, 1970)	16, 17	η_+^{opt}, η_0^{opt}, η_-^{opt}	2–40
Schlachter *et al.* (1969)	18	F_+^∞, F_0^∞, F_-^∞	1–40
Khirnyi and Kochemasova (1970)	19	η_-^{opt}	0.4–12
Meyer and Anderson (1975)	20	F_-^∞	1.5–11.5 [a]
Cisneros *et al.* (1976)	21	F_-^∞	0.5–2.5
Agafonov *et al.* (1976)	22	η_-^{opt}	0.3–12
Girnius *et al.* (1977)	23	F_-^∞	1–6
Girnius *et al.* (1977)	24	F_0^∞	60–400
Schlachter *et al.* (1977, 1979, and present publication)	14, 25 26	F_+^∞, F_0^∞, F_-^∞	0.3–10
Nagata (1979)	27	η_-^{opt}	1.5–10
Nagata (unpublished)	28	F_+^∞, F_0^∞, F_-^∞	2–10
Meyer (unpublished)	29	F_-^∞	0.2–2
Agafonov *et al.* (1980)	30	η_-^{opt}	0.2–12

[a] Also 3–23-keV D_2^+ incident.

get in charge state i is represented by $F_i(\pi)$, where π is the line density or target thickness. For number density n and path length l:

$$\pi = \int_0^l n(x)dx. \tag{3}$$

The equilibrium yield of atoms or ions in charge state i is denoted by F_i^∞, which is independent of π.

$$F_i^\infty = \lim_{\pi\to\infty} F_i(\pi). \tag{4}$$

Many experimenters measure $\eta_i(\pi)$ rather than $F_i(\pi)$, where η_i is the charge-state fraction relative to the incident beam. F_i^∞ is independent of target geometry, while $\eta_i(\pi)$ depends on target geometry; $\eta_i(\pi)$ exhibits a maximum (η_i^{opt}) and goes to 0 as π goes to infinity. This is further discussed in the Appendix.

We assume that the charge-state fraction, $F_i(\pi)$, is a function only of π and of the incident species: $F_i(\pi)$ is the same for any combination of n and l giving the same π, and for any incident beam intensity in the range we considered. This implies

TABLE II. Summary of measurements of equilibrium yields and conversion efficiencies for deuterium ions and atoms in sodium vapor.

Author	Reference	Measured	D energy range (keV)
D'yachkov and Zinenko (1968)	31	F_0^∞, F_-^∞	15–40
D'yachkov *et al.* (1972)	32	η_-^{opt}	3–20
Grüebler *et al.* (1969, 1970)	16, 17	η_+^{opt}, η_0^{opt}, η_-^{opt}	2–40
Dimov and Roslyakov (1974)	33	η_-^{opt}	1.2–20
Schlachter *et al.* (1979) and present publication	26	F_+^∞, F_0^∞, F_-^∞	0.3–10
Nagata (1979)	27	η_-^{opt}	1.5–10
Nagata (unpublished)	28	F_+^∞, F_0^∞, F_-^∞	1.5–10
Anderson *et al.* (1979)	34	F_+^∞, F_0^∞, F_-^∞	2–50
Agafonov *et al.* (1980)	30	η_-^{opt}	0.2–12

either that beam and target excitation are negligible, or that beam and target excitation do not affect the results.

All results referred to will be for deuterium atoms and ions unless explicitly stated otherwise. Over our energy range cross sections and yields measured with hydrogen and deuterium projectiles at the same velocity have been found to be the same;[42] therefore results for H projectiles will be treated as if the experiment had been performed using D, but at twice the energy.

Some preliminary results have been reported in conference proceedings,[14,25,26] including a summary of cross sections and equilibrium yields in metal vapors up to 1977.

II. EXPERIMENTAL APPROACH

A. General method

A fast ion or atom beam traversed a recirculating metal-vapor target of variable thickness. The beam after the target was analyzed in an electric field to determine the D^+, D^0, and D^- charge-state fractions. An overall view of the apparatus is shown in Fig. 1. The geometries required for cross section and for equilibrium-yield measurements are described in detail below.

B. Beam preparation

The ion beam of interest, i.e., D^+, D_2^+, D_3^+, or D^- was directly extracted at full acceleration potential from one of two duoplasmatron ion sources.[43] The ion energy in this type of ion source is very nearly determined by the acceleration potential, which was regulated and measured with an uncertainty of less than 0.1 percent using a precision voltage divider. The difference between the positive and the negative-ion source is that an off-axis extractor is used in the negative-ion source, which limits the extracted electron current. The D^+ or D^- current on target was 1–30 nA.

The extracted beam was focused in an Einzel lens, then steered and 100 percent square-wave modulated at a 50 percent duty cycle by transverse electric fields. The modulated beam was required for the neutral-atom detection. Frequencies between 0.28 and 4.65 Hz were used.

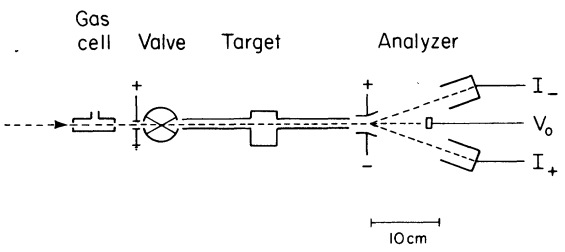

FIG. 1. Schematic diagram of the apparatus. A momentum-selected beam was incident from the left. A voltage applied to the first set of deflection plates swept the charged components from the beam when a D^0 beam, produced in the gas cell, was desired.

Some measurements required an incident D^0 beam, which was produced from D^+ or D^- beams in an argon gas cell located ahead of the target. A transverse electric field was used after the gas cell to remove remaining ions.

Two different experiments required the incident beam to be collimated. The geometries we used are shown schematically in Fig. 2. Geometry Ib was used to test the effects of incident-beam collimation on equilibrium-yield measurements. We used geometry II for cross-section measurements, and Ic and IIa for some equilibrium-yield measurements. Argon gas in the gas cell produced D^0 from incident D^+ or D^-, with remaining ions removed by the deflection plates. Collimator C_5, 0.75-mm diameter, served as a gas-flow impedance (there were pumps located upbeam of C_8 and between C_5 and C_4).

C. Target and analyzer

The recirculating metal-vapor (heat pipe) target[44-47] is shown in Fig. 3. A wick lining the tar-

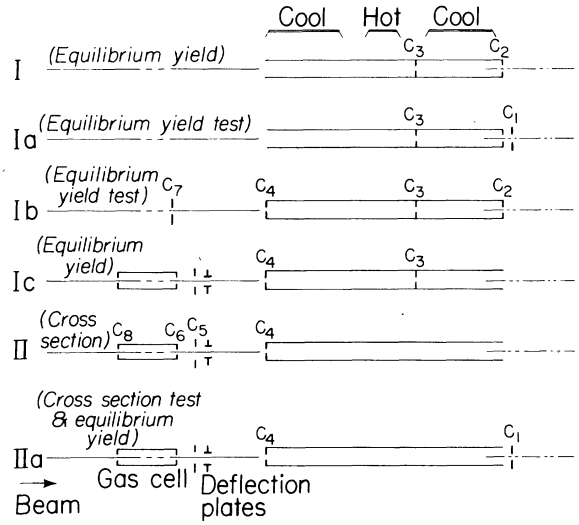

FIG. 2. Schematic diagram of various configurations of the metal-vapor target and beamline showing collimation of incident beam and limiting apertures for scattered beam. The elements labeled C_1–C_8 indicate the positions of apertures for each configuration. Two 0.51-mm-diameter apertures (C_6 and C_4) separated by 9.5 cm collimated the beam for cross-section measurements, while C_5 and C_8 (0.76 mm) served as pumping impedences. C_3 and C_2 (2.8 and 7.9 mm) limited the exit divergence for equilibrium measurements (separation, 9.2 cm). Some equilibrium measurements were made using geometries Ic and IIa.

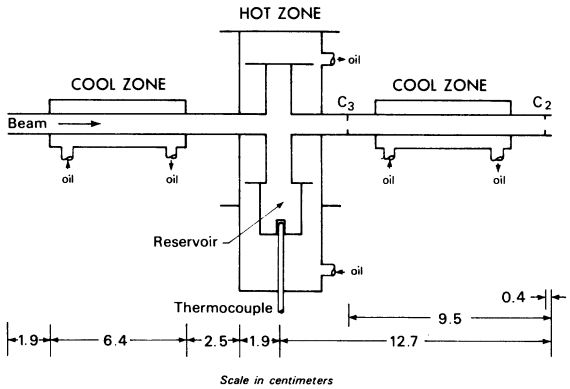

FIG. 3. Metal-vapor target, showing the relative positions of the oven and liquid-metal-recovery components. Dimensions are in cm.

get[48] wall returns most escaping atoms to the central reservoir zone containing the liquid metal. The temperature of the center portion was controlled by a rapidly circulating hot oil bath[49] (up to 250 °C) or a quartz-lamp furnace for higher temperatures. The ends of the tube away from the central portion were maintained just above the melting point of the target material (e.g., 31 °C for cesium) by another circulating oil system. The entire assembly was made of 304 stainless steel except for the vacuum gaskets which were of oxygen-free copper.[50]

The target density was variable from a few times 10^{10} atoms/cm^3 to greater than 1×10^{16} atoms/cm,^{3} which was inferred by the use of vapor-pressure tables[51] from the temperature as measured by a chromel-alumel thermocouple located in a well in the target. Overall length of the target was 25.4 cm; the length of the hot central zone was 3.8 cm; the inner diameter was 0.95 cm.

The beam leaving the target was analyzed by a transverse electric field. The analyzer was as closely coupled to the target as possible in order to measure divergent beams. The positive and negative beams were deflected electrostatically into magnetically suppressed Faraday cups while the neutral beam was collected on the front face of a pyroelectric detector. The front of each Faraday cup was approximately 14.5 cm from the target exit, and the front face of the neutral-atom detector about 11.4 cm from the target exit. Calculations of ion trajectories were used to suitably position the electric-field deflection plates. Calculations of electric-field penetration into the target showed that the electric field did not perturb ion trajectories inside the target.

D. Beam detection and data acquisition

The charged particles were collected on a pair of 2.8-cm diameter shielded Faraday cups with transverse magnetic fields to suppress secondary-electron emission. The resulting current was measured on a pair of sensitive electrometers which were periodically calibrated using a constant-current source. The magnetic suppression of the Faraday cups was checked by applying positive bias to the cups in order to electrostatically suppress secondary electrons; the current was unchanged to within the reading accuracy (< 1 percent).

The neutral-particle detector was a pyroelectric[52,53] lead-zirconate-titanate ceramic disc[54] with a thin silver coating on each face.[55] The front face was grounded and the signal was taken from a shielded connection at the back. In the absence of any current drain, the voltage at the back was proportional to the temperature of the device.[52] The discs we used were 2.5-cm diameter and 1.25-mm thick, and had a capacitance of ~ 50 μf. Since the beam was chopped, an ac voltage was developed which was detected with a lock-in amplifier having 10^8-ohm input impedance. This system developed about 10 V per watt at 1 Hz and allowed us to measure beams as small as 10^{-7} watts (e.g., 10^{-10} ampere at 1 keV).

Since the neutral detector is not sensitive to electric charge it was a simple matter to calibrate it with the ion beam. The response of the ceramic was measured before and after each run. The neutral-detector sensitivity K, is the pyroelectric voltage divided by the total beam current incident on it (measured by a Faraday cup) and divided by the beam energy. A series of measurements of the detector sensitivity K, made over a period of months at different energies, is shown in Fig. 4. This series of measurements corresponds to the F_i measurements in rubidium, all of which were made with Gulton G1500 pyroelectric-ceramic material, with 100 percent modulation of the beam at 2.27 Hz. The lack of energy dependence indi-

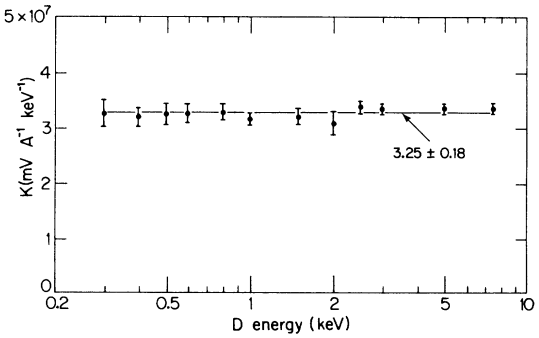

FIG. 4. Calibration constant, K, of the pyroelectric neutral-beam detector, as a function of beam energy E. These data are for G1500 ceramic at 2.27-Hz modulation frequency.

cates that surface charging did not occur and that reflected energy is small. The lack of time dependence (not shown) indicates long-term stability.

The method of acquiring data was to simultaneously integrate the output of the electrometers and the lock-in amplifier for a period several times longer than the instrumental time constants, while holding the target temperature constant. This method allowed us to filter out noise and short-term beam drift. After sufficient time (typically 1 minute), the integration was stopped. The ratio of the charge accumulated for each beam component to the total gave the fraction of each component. Since the long-term drift of the beam was small, the total beam leaving the target compared to the initial total beam for thin targets gave a good measure of beam loss as a function of target density.

E. Geometric considerations and scattering

The requirements on target geometry are different for measuring cross sections and for measuring equilibrium yields. The basic geometric considerations are shown in Fig. 5. For equilibrium-yield measurements we assumed that nearly all the particles had undergone several scattering and charge-changing collisions, so that the profile of each charge species taken at the exit of the target would show the same distribution. Because of this, we collimated the beam after it emerged from the hot zone of the target so that no beam particle could find its way past the exit collimator and miss the neutral detector. Since the Faraday cups subtend a larger solid angle than the neutral detector, we were certain of being able to collect an equal proportion of all three charge-state beams. To test that one charge species does not have a different profile than the others, we made some measurements with a reduced exit aperture by inserting a 1-mm diameter aperture after the target (C_1 in geometry Ia as shown in Fig. 2). The F_i^∞ results were the same with and without C_1 in place. We also made several F_i^∞ measurements with a collimated incident beam (geometry Ib in Fig. 2); the incident beam was limited to a half-angle divergence of 0.31° by C_4 and C_5, each 0.60-mm diameter separated by 11.0 cm. The F_i^∞ results were also the same to within experimental uncertainties.

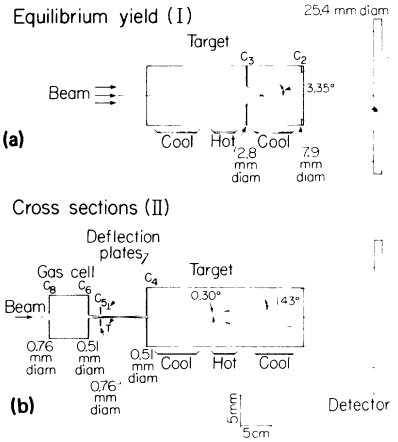

FIG. 5. Details of collimation and scattering geometry. (a) shows the primary configuration for equilibrium-yield measurements (geometry I of Fig. 2). The rays show the maximum angle at which particles may exit the target. (b) shows the configuration for cross-section measurements (geometry II of Fig. 2). The rays show the minimum angle within which all particles scattered at the center of the oven will be detected. Particles scattered from different locations may reach detectors after undergoing larger-angle scattering collisions. Note that the vertical scale is 10 times the horizontal scale.

We used geometries I, Ic and IIa for most of the F_i^∞ measurements. Geometry I has C_3 with 2.85-mm diameter, C_1 with 7.94-mm diameter, the half-angle for scattered beam was 3.35°. Geometry Ic was without C_2, so the beam was limited by the 9.52-mm-diameter target exit, with a half-angle for scattered beam of 3.72°; the maximum beam diameter on the neutral detector was 2.41 cm, the largest of any of these geometries. We also used geometry IIa, for which C_1 had a diameter of 3.97 mm, which limited the scattered beam to a half-angle divergence of 3.74°; the maximum beam diameter on the neutral detector was 1.65 cm. We obtained the same results for F_i^∞ with each of these geometries to within experimental uncertainties, which we expected, since in all cases the scattered beams were smaller than the detectors.

For cross-section measurements, where fewer than 10 percent of the incident particles undergo even one charge-changing collision, the considerations are more familiar. In this case, we want to be certain that negligibly few scattering collisions take place which result in loss of particles before reaching the detectors. Therefore, the beam was collimated to a small diameter with little divergence before it entered the oven. The exit apertures were removed to allow all particles scattered within 1.4° to be collected, and most particles scattered as much as 2° to be collected. This is shown as geometry II in Fig. 2, with detailed scattering shown in Fig. 5. Collimators C_6 and C_4, 0.5-mm diameter separated by 9.5 cm, limited the incident beam to 0.30°, with a maximum beam diameter at the center of the target (with no scattering) of 1.86 mm. This allowed an additional scattering of 1.43° (in the worst case) to exit the

target and be detected. (The usual method of specifying target acceptance is the half angle from the axis at the center of the target to the target exit, or 2.15° in our case).

The angular acceptance set a lower energy limit for cross-section measurement for a given geometry. We tested our cross-section measurements by inserting a 3.97-mm-diameter aperture C_1 at the target exit (geometry IIa, effectively halving the angular acceptance, to test for large-angle scattering. Any cross section which changed by more than 5 percent was rejected. We found that neither σ_{0-} nor σ_{-0} changed by 5 percent when aperture C_1 was inserted, which is consistent, for σ_{0-}, with recent calculations by Olson[40]; he calculated that, for our geometry, we would collect 95 percent of the scattered beam for H^0 incident on cesium down to an energy of about 0.5 keV.

F. Measurement procedure

1. Equilibrium yields

Thick-target measurements were made using the geometry shown in Fig. 5a, or one similar (geometries I, Ic, II(a) in Fig. 2) except for the test geometries already described (I(a) and I(b) in Fig. 2).

Before each run the incident beam (D^+ or D^-) was slowly swept across the neutral detector and the Faraday cups, using the analysis-plate voltage, to check for uniform sensitivity of the pyroelectric-ceramic disc, and to determine the analysis voltage required to center the ion beams in the Faraday cups. The neutral-atom detector was then calibrated by making a series of constant-time-interval measurements with the ion beam alternately on the neutral detector and on the Faraday cups. Beam intensity fluctuations and noise were sufficiently small to allow calibration to better than 95 percent accuracy The calibration constant was compared with previous runs made with the same detector and frequency to discover any detector problems which might be present (due to target material buildup on the detector face, for example, which would increase the thermal response time). This same procedure was followed after each run to recheck neutral-detector calibration and response.

The central region of the target was then heated while the target temperature was monitored using a chromel-alumel thermocouple embedded in the target reservoir (Fig. 3). The data were accumulated after observing a steady temperature for about one minute or longer.

A complete equilibrium-fraction determination consisted of a set of these measurements at different target temperatures. Figures 6 and 7

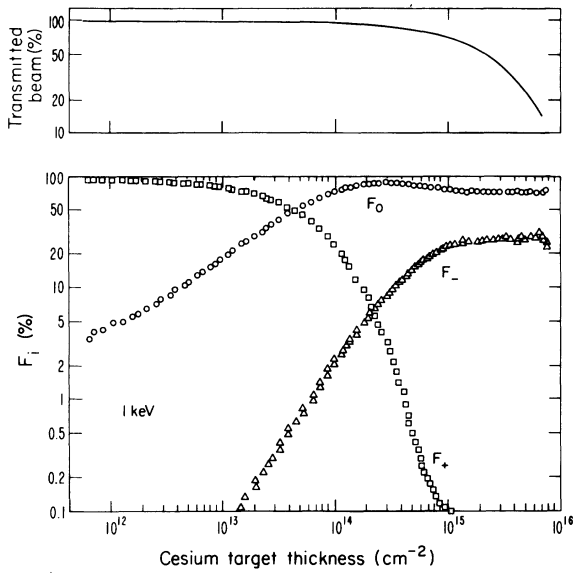

FIG. 6. Charge-state fractions, F_i, as a function of cesium-target thickness, π, for 1-keV D^+ incident on cesium vapor. Note (Figs. 6–8): Fractions shown for π less than equilibrium are not accurate because of unequal collection of scattered beams; the data are shown to illustrate the plateau in F_i at large values of π.

show $F_i(\pi)$ for 1-keV D^+ incident on cesium vapor and for 2-keV D^+ incident on sodium vapor. Figure 6 also shows total relative beam intensity as a function of target thickness. We found in all measurements a plateau in the charge-state fractions for temperatures sufficiently high, indicating charge-state equilibrium. An increase in target density by a factor as large as 5 caused no change

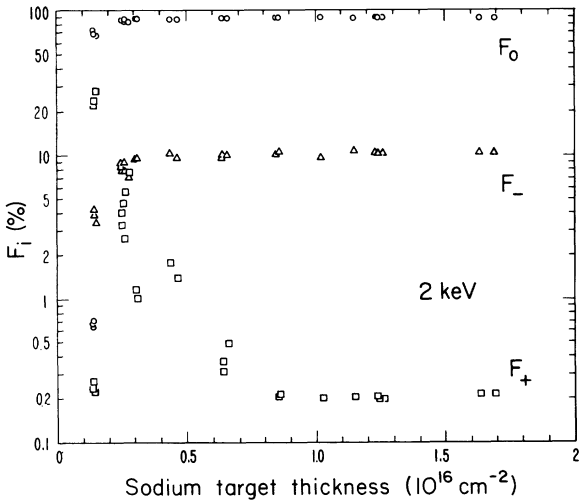

FIG. 7. Charge-state fractions, F_i, as a function of sodium-target thickness, π, for 2-keV D^+ incident on sodium vapor. See note in Fig. 6.

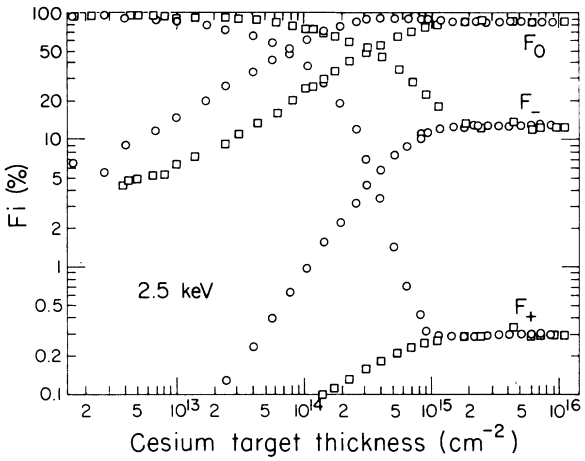

FIG. 8. Charge-state fractions, F_i, as a function of cesium-target thickness, π, for 2.5-keV D^- (□) and 2.5-keV D^+ (○) incident on cesium vapor. See note in Fig. 6.

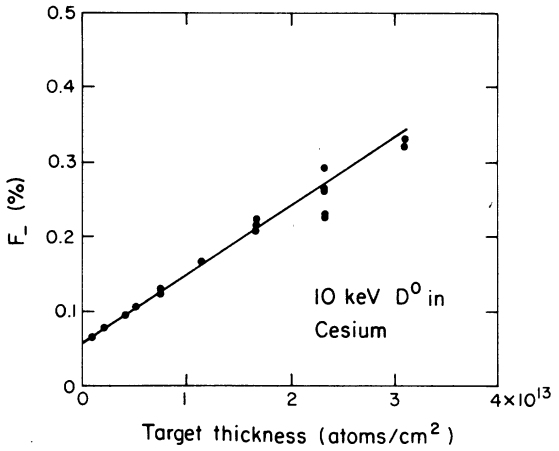

FIG. 9. Thin-target values of $F_-(\pi)$ for 10-keV D^0 incident on cesium vapor. These data were used to determine σ_{0-}.

in the observed fractions. We also found, for D^+ incident on cesium vapor at low energies, that $F_0(\pi)$ had a broad maximum at intermediate target thicknesses, arising from the large value of $\sigma_{+0}(\sim 10^{-14}$ cm^2), so that the incident D^+ is largely converted to D^0 for $\pi \sim 1-2\times10^{14}$ cm^{-2}, while a much thicker target is required for appreciable D^- formation and for charge-state equilibrium.

Figure 8 shows $F_i(\pi)$ for 2.5-keV D^- and 2.5-keV D^+ incident on cesium vapor. The asymptotic values of the charge-state fractions are independent of the incident-ion species.

We found it easier in some cases to fix the target temperature and vary the beam energy. We were careful in such cases to measure the neutral-detector response at different energies and to have a target thickness sufficient for equilibrium at all the energies in the range.

2. *Cross sections measurements*

Thin-target measurements were made using a pre-collimated beam, as shown in Fig. 5(b) (geometry II in Fig. 2), and were tested using geometry IIa in Fig. 2. The procedures were the same as for equilibrium measurements except that the temperatures were kept low enough so that the incident species was attenuated by less than 10 percent, and more care was exercised to accurately determine the target thickness.

It was usually helpful to overheat the oven at least once before making any measurements. In this way sufficient target metal was distributed throughout the oven so that vapor pressures in equilibrium with the temperatures established themselves rapidly throughout, giving a unique function of π vs temperature. The other important factor in determining π accurately was to change target temperature in small steps, with each change followed by a sufficient time for gradients to adjust. We estimate that π could be repeated to within 5 percent, whereas the absolute determination of π is only within 25 percent due to uncertainty in the temperature measurement, vapor-pressure tables, and the effective length determination of the target.

The cross sections were determined by fitting a straight line to the growth curves of the product species, corrected for attenuation over ranges of π where the attenuation of the incident specie was less than 10 percent and where no secondary process contributed as much as 10 percent to any single measurement. The cross section was determined from the slope of the growth curve to within our statistical uncertainty (usually about 5 percent or less). Figure 9 shows thin-target $F_-(\pi)$ for 10-keV D^0 incident on cesium vapor. We determined σ_{0-} from these data.

G. Analysis of uncertainties

The primary source of uncertainty for the equilibrium-yield measurements is the calibration of the neutral-atom detector. Although individual measurements varied, we combined measurements of the sensitivity for different energies and times to obtain an average calibration uncertainty of 3–6 percent. The uncertainty in relative calibration of electrometer and lock-in amplifier scales was about 3 percent. The third source of uncertainty results from the statistics of the measurement itself, i.e., in obtaining the plateau value of F_i^∞. This ranged from less than 1 percent to as high as 10 percent, but was typically 1–4 percent.

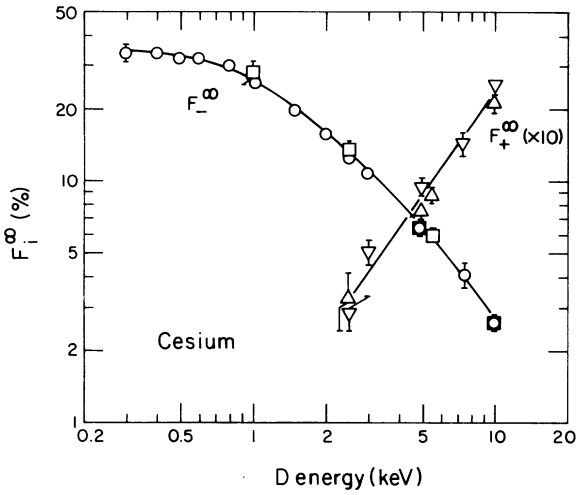

FIG. 10. Equilibrium yields, F_-^∞ and F_+^∞, for D in cesium vapor. F_+^∞ results are multiplied by 10. The lines are shown for clarity. Yields for incident D^+ are shown by ○ and ▽; yields for incident D^- are shown by □ and △.

These three sources of uncertainty were added in quandratures to obtain the overall uncertainty for a given series of measurements. Finally, weighted averages were calculated for all equivalent equilibrium measurements, between two and five measurements for each energy and target, to obtain the results shown in Figs. 10–12 and in Table III. Uncertainties in F_-^∞ are typically 3–5 percent; uncertainties in F_+^∞ are larger because of smaller signal levels.

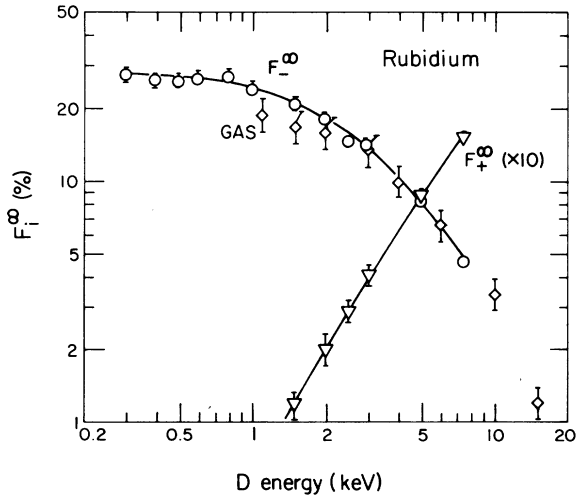

FIG. 11. Equilibrium yields, F_-^∞ (symbol ○) and F_+^∞ (symbol ▽), for D in rubidium vapor. F_+^∞ results are multiplied by 10. Also shown are the F_-^∞ results of Girnius *et al.* (Ref. 23) (labeled GAS, symbol ◇). The lines are shown for clarity.

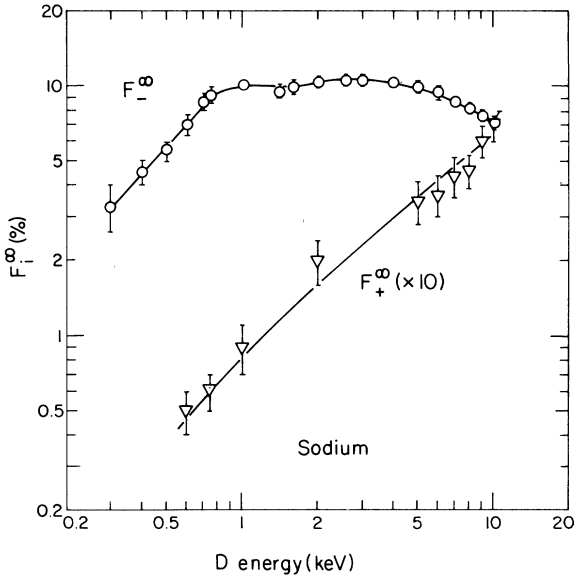

FIG. 12. Equilibrium yields, F_-^∞ and F_+^∞, for D in sodium vapor. F_+^∞ results are multiplied by 10. The lines are shown for clarity.

The same considerations as above apply to the relative cross-section measurements. Absolute uncertainty must also include the uncertainty in the effective length of the hot portion of the target, the temperature measurement, and the vapor-pressure data. For low-temperature cesium vapor[56] the target length was 5.3 ± 0.7 cm, based on the geometry of the target. The effective length and associated uncertainty are the result of considering two extreme choices which we expect to bracket the actual effective length by an ample margin. The maximum possible effective length would result if no cesium could stick to the walls of the 2.5-cm-long transition region between the 3.8-cm-long hot zone in the center and the cold zone at each end of the target. This nonphysical extreme would result in conditions resembling a gas cell which, for molecular flow, is closely approximated by a uniform density gradient from the hot zone to the cold zone. (We assume nearly 100% sticking of the cesium vapor to the walls of the cold zone.) Thus the maximum effective path length at the density of the center section is 6.3 cm. The minimum length model assumes that the density along the transition region is determined solely by the wall temperature. We also assume a uniform temperature gradient in this region. The integral of the density over this path length (Eq. 3) yields an effective minimum length at the density of the center section of 4.2 cm. The cited effective length is the average of these two extremes and the uncertainty is taken to be 70% of the maximum variation. We checked

TABLE III. Equilibrium yields F_+^∞, F_0^∞, and F_-^∞, for D in cesium-, rubidium-, and sodium-vapor targets, and cross sections, [a] σ_{0-} and σ_{-0}, for D^0 and D^- in cesium vapor.

D energy (keV)	Cesium F_-^∞ (%)	Cesium F_0^∞ (%)	Cesium F_+^∞ (%)	Rubidium F_-^∞ (%)	Rubidium F_0^∞ (%)	Rubidium F_+^∞ (%)	Sodium F_-^∞ (%)	Sodium F_0^∞ (%)	Sodium F_+^∞ (%)	Cesium σ_{0-} (10^{-16} cm^2)	Cesium σ_{-0} (10^{-16} cm^2)
0.3	33.9 ±2.6	66.1 ±2.6		27.7 ±1.9	72.3 ±1.9		3.3 ±0.7	96.7 ±0.3			
0.4	33.8 ±1.4	66.2 ±1.4		26.3 ±1.7	73.7 ±1.7		4.5 ±0.5	95.5 ±0.5			
0.5	32.3 ±1.3	67.7 ±1.3		26.0 ±1.6	74.0 ±1.6		5.5 ±0.5	94.5 ±0.5			
0.6	32.3 ±1.4	67.7 ±1.4		26.7 ±1.8	73.7 ±1.8		7.0 ±0.7	93.0 ±0.7	0.05 ±0.01		
0.7							8.7 ±0.7	91.3 ±0.7			
0.75							9.2 ±0.7	90.7 ±0.7	0.06 ±0.01		
0.8	30.2 ±1.3	69.8 ±1.4		27.3 ±1.7	72.7 ±1.7	<0.06					
1.0	26.1 ±1.4	73.9 ±1.4		24.3 ±1.5	75.6 ±1.5	<0.08	10.1 ±0.5	89.8 ±0.5	0.09 ±0.02		
1.4							9.6 ±0.6	90.3 ±0.6			
1.5	19.8 ±0.7	80.1 ±0.8	<0.2	20.9 ±1.2	79.0 ±1.2	0.12 +0.012 −0.020					
1.6							9.9 ±0.6	90.0 ±0.6			
2.0	15.8 ±0.7	84.1 ±0.8	<0.25	18.2 ±1.1	81.6 ±1.1	0.20 ±0.03	10.4 ±0.5	89.4 ±0.4	0.20 ±0.04		
2.5	12.8 ±0.4	86.9 ±0.4	0.30 ±0.05	14.7 ±0.7	85.0 ±0.7	0.29 ±0.03				3.7(±0.2, ±0.9)	23(±1, ±6)
2.6							10.6 ±0.5	89.1 ±0.6			
3.0	10.9 ±0.5	88.6 ±0.6	0.51 ±0.08	14.2 ±0.7	85.4 ±0.8	0.41 ±0.04	10.6 ±0.5	89.1 ±0.6			
4.0							10.4 ±0.5	89.3 ±0.6			
5.0	6.46 ±0.20	92.6 ±0.3	0.89 ±0.08	8.24 ±0.36	90.9 ±0.4	0.86 ±0.06	10.0 ±0.5	89.6 ±0.6	0.35 ±0.07		30(±1, ±8)
5.5	5.94 ±0.40	93.2 ±0.5	0.87 ±0.12							1.8(±0.1, ±0.5)	31(±1, ±8)
6.0							9.5 ±0.6	90.1 ±0.7	0.37 ±0.07		
7.0							8.8 ±0.4	90.8 ±0.5	0.44 ±0.08		
7.5	4.12 ±0.45	94.4 ±0.6	1.44 ±0.16	4.67 ±0.20	93.8 ±0.3	1.52 ±0.08					
8.0							8.3 ±0.4	91.2 ±0.5	0.46 ±0.07		

TABLE III. *(Continued)*

D energy (keV)	Cesium F_-^∞ (%)	Cesium F_0^∞ (%)	Cesium F_+^∞ (%)	Rubidium F_-^∞ (%)	Rubidium F_0^∞ (%)	Rubidium F_+^∞ (%)	Sodium F_-^∞ (%)	Sodium F_0^∞ (%)	Sodium F_+^∞ (%)	Cesium σ_{0-} (10^{-16} cm^2)	Cesium σ_{-0} (10^{-16} cm^2)
9.0							7.8 ±0.4	91.6 ±0.5	0.61 ±0.09		
10.0	2.65 ±0.08	95.0 ±0.2	2.39 ±0.08				7.2 ±0.5	92.1 ±0.6	0.71 ±0.10	0.94(±0.04, ±0.24)	37(±2, ±9)

[a] Relative and absolute uncertainties are shown, respectively.

our target length by measuring σ_{+0} for 5-keV D^+ in cesium vapor, obtaining a cross section of 8.5×10^{-15} cm^2, which compares well with the result of Meyer and Anderson.[57] All of these sources of error add an independent 25 percent uncertainty to the absolute cross-section results. Both relative and absolute cross-section uncertainties are shown in Fig. 16 and in Table III.

III. RESULTS AND DISCUSSION

A. Equilibrium yields: Results

Equilibrium-yield results F_+^∞, F_0^∞, and F_-^∞ are shown in Table III for deuterium beams which emerge from thick targets of cesium, rubidium, and sodium vapors. The positive and negative equilibrium yields are shown graphically in Figs. 10–12. Notable are the high negative-ion yields for cesium and rubidium at energies less than 1 keV deuterium energy, which are as large as 34 percent for cesium at 300 eV. The D^- yield in sodium vapor has an interesting feature between 1 and 2 keV. This short flat spot suggests that the electron-capture mechanism may change at 1–2 keV.

The results are compared, together with those for deuterium in magnesium[58] and strontium[59] vapors, in Fig. 13. The negative-ion yields in cesium and rubidium appear quite similar, which probably results from the near equality of the binding energy of the outer electron on each, 3.89 eV for cesium and 4.18 eV for rubidium. The yield in sodium is interesting in that it exceeds the yields of cesium and rubidium at energies greater than 4 keV.

We made a few measurements using D_2^+ and D_3^+ as projectiles incident on cesium- and sodium-vapor targets, to check whether D_2^+ or D_3^+ might give a greater D^- yield per deuteron at thinner targets than at equilibrium. We discovered no enhancement. F_-^∞ per deuteron is the same for D^+, D^-, D_2^+, and D_3^+ projectiles at the same energy per deuteron. The target thickness required to dissociate D_2^+ or D_3^+ and to reach charge-state equilibrium was an order of magnitude greater than for D^+ or D^- incident,[60] for both cesium- and sodium-vapor targets.

Previously reported results for F_-^∞ in cesium[61] are compared with our results in Fig. 14(a). A related quantity η_-^{opt} is shown in Fig. 14 (b) and is also compared with our results. η_-^{opt} is the peak negative-ion yield as compared with the incident flux; it is necessarily geometry dependent. The same comparisons are made in Figs. 15(a) and 15 (b) for the sodium-vapor results. Figure 11 compares our F_-^∞ results with those of Girnius *et al.*[23] for rubidium. The most noticable point in the comparisons is that the more different sets of results there are, the greater and more numerous are the discrepancies; the worst case is for cesium-vapor targets, while in rubidium vapor the two experiments agree to within their stated uncertainties. The other notable point is that η_-^{opt} measurements particularly in sodium are not generally lower than F_-^∞ measurements, as one would expect.

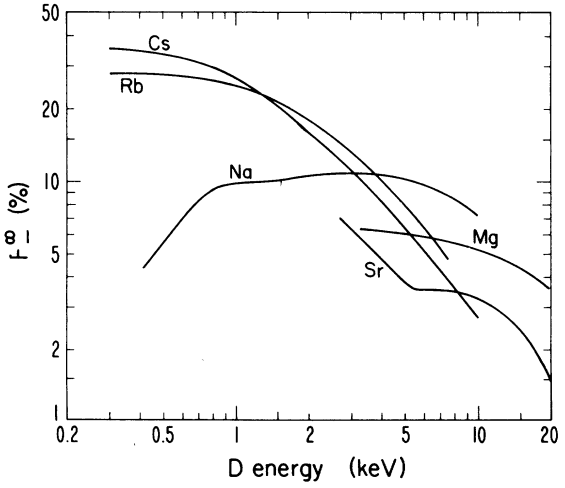

FIG. 13. Equilibrium yield, F_-^∞, for D in cesium-, sodium-, rubidium-, (Ref. 58) magnesium-, and (Ref. 59) strontium-vapor targets.

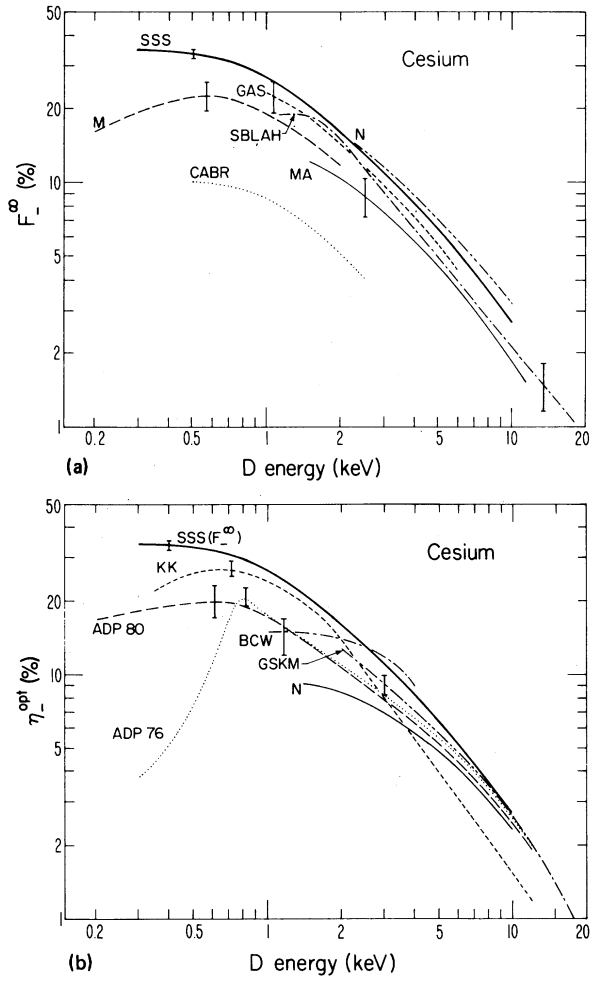

FIG. 14. Equilibrium yield, F_-^∞ (a), and optimum negative-ion conversion efficiency, η_-^{opt} (b), for D in cesium vapor. Heavy line labeled SSS (present F_-^∞ results), M (Meyer, Ref. 29), GAS (Girnius *et al.*, Ref. 23), SBLAH (Schlachter *et al.*, Ref. 18), N (Nagata, Refs. 27 and 28), MA (Meyer and Anderson, (Ref. 20), CABR (Cisneros *et al.*, Ref. 21), KK (Khirnyi and Kochemasova, Ref. 19), ADP76 (Agafonov *et al.*, Ref. 22), ADP80 (Agafonov *et al.*, Ref. 30), GSKM (Grüebler *et al.*, Refs. 16 and 17), and BCW (Bohlen *et al.*, Ref. 15). Typical uncertainties are shown.

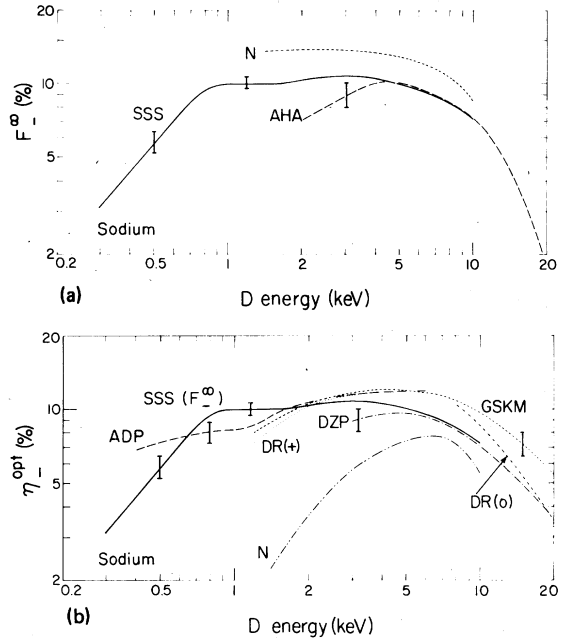

FIG. 15. Equilibrium yield, F_-^∞ (a), and optimum negative-ion conversion efficiency, η_-^{opt} (b), for D in sodium vapor. Heavy line labeled SSS (present F_-^∞ results), N (Nagata, Refs. 27 and 28), AHA (Anderson *et al.*, Ref. 34), ADP (Agafanov *et al.*, Ref. 30), GSKM (Grüebler *et al.*, Refs. 16 and 17), DZP (D'yachkov *et al.*, Ref. 32), and DR (Dimov and Roslyakov, Ref. 33; + and 0 indicate incident D^+ and D^0). Typical uncertainties are shown.

B. Equilibrium yields: Discussion

A common difficulty encountered when measuring equilibrium yields at low energy is the necessity of measuring the neutral-atom flux. Many authors employ a secondary-electron-emission detector[62,63] for this purpose. Calibration of the detector can be difficult since it requires a known flux of neutral atoms at the appropriate energy. To overcome this difficulty, some experiments invoke previous measurements[64] which show a constant ratio between secondary-electron emission due to incident D^+ as compared to D^0. Whether this assumption is justified or not, a further complication arises as the emitting surface becomes contaminated with the target material, which changes the secondary-electron-emission coefficient[65] during the course of an experiment. With these difficulties in mind, it is not surprising to see large differences in the results, especially at lower energies where it is difficult to obtain an independently calibrated neutral beam. This is perhaps the reason for so many η_-^{opt} measurements since, in these cases, it is not necessary to measure the neutral-atom flux.

Another difficulty which may arise is failure to achieve sufficient target thickness for equilibrium. This could result from loss of signals due to beam attenuation, or to unwillingness to increase target thickness to avoid excessive loss of target material from the oven. Finally, we address the possibility that differences might be accounted for by physical effects: target excitation, beam excitation, or polymerization within the target.

Target excitation. Excitation of the cesium valence electron to the $6p$ state could enhance

electron capture, i.e., we would expect the relation (at low energy)

$$\sigma(D^0+Cs(6p)\rightarrow D^-+\cdots) > \sigma(D^0+Cs(6s)\rightarrow D^-+\cdots) \quad (5)$$

to be true because of the reduced ionization potential of the $6p$ state. $Cs(6p)$ decays rapidly by electric-dipole radiation to $Cs(6s)$. However, because of radiation trapping, a population of $Cs(6p)$ sufficient to affect the measurements might result. Pradel *et al.*[66] measured cesium density by absorption of the 8521 Å line; we estimate that the $Cs(6p)$ population is less than 1 part in 10^6 at a density of 10^{15} cm^{-3}, which would be far too small to have any effect. That we obtained the same values of F_i^∞ for a wide range of beam intensities confirms this conclusion. We would expect the other targets to behave similarly.

Beam Excitation. A large population of D^0 in excited states might be expected to reduce the D^- yield, since D^- exists only as $D^-(1s^2)$. However the data of Pradel *et al.*[67] and Schlachter *et al.*[68] indicate that for 1-keV D^+ in cesium vapor, the fraction of metastable D(2s) in the beam for $\pi \sim 1 \times 10^{15}$ cm^{-2} is too small to have any effect. The $D(2p)$ state must also be depopulated, since the depopulation of the $2s$ state is principally through collisional mixing of the $2s$ and $2p$ states followed by radiative decay of $D(2p)$ to $D(1s)$ ($\sim 10^{-9}$ sec). Again, we would expect other targets to behave in a similar manner.

Polymers. There is some evidence that the D^- yield from passage of a beam through a solid gives an enhanced D^- yield relative to passage through a vapor of the same metal.[69] Polymers in the target might produce a similar effect. However, under the conditions encountered in the present experiment, the cesium or rubidium polymer fraction is less than 1 percent,[70] while in sodium,[71] it does not exceed 3 percent. This is too small to affect the results.

C. Cross sections

Results for the cross sections σ_{0-} and σ_{-0} for D^0 and D^- in cesium vapor at 2.5 to 10 keV are shown in Fig. 16 along with other experimental and theoretical results. We have multiplied the results of Leslie *et al.*[35] by a factor of 2.0 to take into account more recent σ_{+0} measurements than those to which they normalized; this also brings their results into better agreement with the higher energy absolute measurements of Girnius *et al.*[24] Our results for σ_{-0} are in fair agreement with the renormalized results of Leslie *et al.*

Our σ_{0-} measurements are consistent with those of Schlachter *et al.*[18] and those of Nagata,[39] given

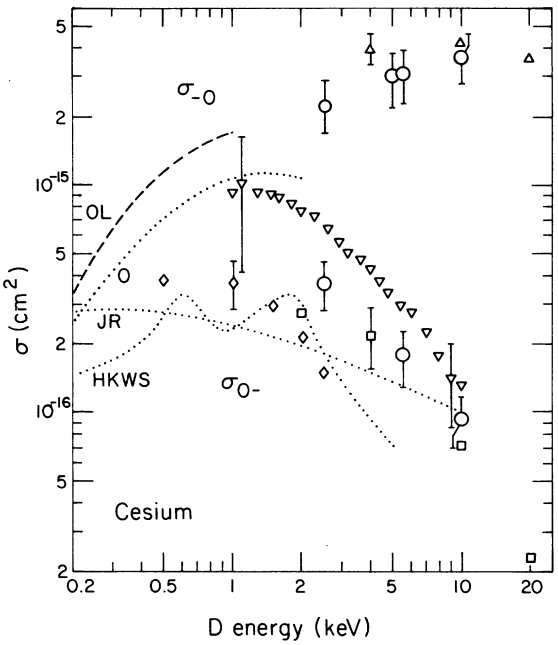

FIG. 16. Cross sections σ_{0-} and σ_{-0} for deuterium in cesium vapor. The open circles are the present results; the symbol size represents relative uncertainty, the error bar represents absolute uncertainty. The results of other experiments, as well as typical absolute uncertainties, are shown: △, Leslie *et al.*, Ref. 35 (renormalized); ▽, Nagata, Ref. 39; □, Schlachter *et al.*, Ref. 18; ◇, Cisneros *et al.*, Ref. 21; Olson and Liu's calculation (Ref. 41) for σ_{-0} is shown as a dashed line (OL). The three calculations of σ_{0-} are shown as dotted lines: HKWS (Hiskes *et al.*, Ref. 37), JR (Janev and Radulović, Ref. 38), and O (Olson, Ref. 40).

the large uncertainties in all three measurements. The results of Cisneros *et al.*[21] are considerably lower than ours.

There have been several recent calculations of σ_{0-} for D^0 in cesium vapor with which experimental results can be compared. These calculations are also shown in Fig. 16. Hiskes *et al.*[37] made a two-state perturbed-stationary-state calculation with straight-line trajectories using adiabatic potentials derived from pseudopotential calculations; they used coupling-matrix elements obtained from *ab initio* calculations of Olson, Shipsey, and Browne.[36] Janev and Radulović[38] used an improved multichannel Landau-Zener method based on work by Ovchinnikova; they used simple diabatic potentials and coupling-matrix elements computed using Janev's asymptotic approximation. Olson[40] has recently performed a quantum-mechanical calculation using diabatic potentials which, when diagonalized with coupling-matrix elements, reproduced the RKR (Rydberg-Klein-Rees) spectroscopic values. Higher-lying states were added

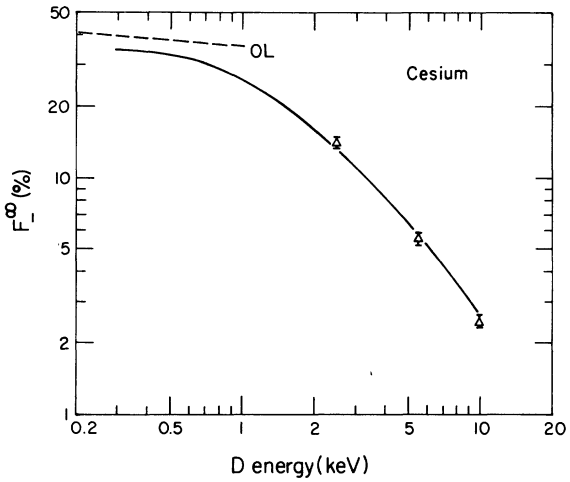

FIG. 17. F_-^∞ calculated from the cross sections for deuterium in cesium, compared with experiment. Solid line, present experimental results; dashed line, F_-^∞ calculated from Olson and Liu's theoretical cross sections. Triangles, F_-^∞ calculated from our experimental cross sections.

using an approximate Landau-Zener method. Our experimental results for σ_{0-} fall between the various theoretical calculations.

The only theoretical calculation of σ_{-0} for D^- in cesium vapor of which we are aware is a recent calculation by Olson and Liu,[41] also shown in Fig. 16. Olson and Liu used a procedure derived from a two-state perturbed-stationary-state cross-section calculation using *ab initio* potential-energy curves for the NaH^- system. They scaled these results to the CsH^- system by correcting for the energy defect and alkali dipole polarizability of the CsH^- system. They conclude that electron transfer is the dominant electron-loss mechanism at low energies, with only a small contribution from molecular ionization. At high energies, however, they point out that direct impact ionization is the dominant mechanism of electron loss. They attribute the large value of σ_{-0} to the long-range nature of the interaction, with impact parameters of $15a_0$ contributing to the cross section. The theoretical calculation of Olson and Liu gives results which appear to agree very well with an extrapolation of the present experimental results.

The equilibrium charge-state fractions can be compared with cross sections.[72] If we neglect the small contribution due to D^+, we can use the relationship

$$F_-^\infty \simeq \frac{\sigma_{0-}}{\sigma_{0-}+\sigma_{-0}} \tag{6}$$

to compare our direct equilibrium-yield measurements with cross-section measurements. This ratio depends only upon relative uncertainties in the measurements, which are much smaller than the absolute uncertainties. In Fig. 17 we show this comparison using our measured cross sections[73] and the theoretical cross sections of Olson,[40] and Olson and Liu.[41] It is gratifying to note the good agreement between results obtained by entirely different methods.

ACKNOWLEDGMENTS

We would like to thank Dr. M. Bacal for bringing the heat-pipe target concept to our attention, Dr. G. P. Lawrence, Dr. R. A. Hardekopf, and Dr. W. Reichelt for useful discussion of their experiences with such targets, and Dr. J. E. Deverall and Dr. W. A. Rankin both for useful discussions and for fabrication of the target. We would like to thank Dr. J. R. Hiskes and Professor L. W. Anderson for many stimulating conversations. We acknowledge the skillful technical assistance of L. A. Biagi, H. A. Hughes, and members of their groups, and C. M. Garrett for his assistance with the electronics. We also acknowledge the assistance of Dr. L. Soroka with computer calculations, and the interest of Dr. R. V. Pyle and Dr. K. H. Berkner. We would also like to thank Dr. T. Nagata, and Dr. B. A. D'yachkov for kindly providing us with their results before publication. Finally, we thank Dr. F. W. Meyer and Dr. R. E. Olson for many stimulating conversations, and for providing us with their results in advance of publication. This work was supported by the Fusion Energy Division of the U.S. Department of Energy under Contract No. W-4705-ENG-48.

APPENDIX: EQUILIBRIUM YIELD AND CONVERSION EFFICIENCY

Let $F_i(\pi)$ represent the fraction of the beam in charge state i at the exit of a target of line density π. Then

$$F_i(\pi) = I_i(\pi)/\sum I_j(\pi)\,, \tag{A1}$$

where $I_i(\pi)$ is the intensity of the component in charge state i. Hence

$$\sum F_i(\pi) = 1\,. \tag{A2}$$

We define the equilibrium fraction in charge state i:

$$F_i^\infty = \lim_{\pi\to\infty} F_i(\pi)\,. \tag{A3}$$

In practice, there exists some value of $\pi = \pi_t < \infty$ such that $F_i(\pi_t)$ is the same as F_i^∞ within measurability.

A quantity related to $F_i^\infty(\pi)$ is $\eta_i(\pi)$, where

$$\eta_i(\pi) = I_i(\pi)/I_0 \tag{A4}$$

and I_0 is the intensity of the beam incident on the target. Owing to scattering losses in the target,

$$\lim_{\pi\to\infty} \eta_i(\pi) = 0 . \tag{A5}$$

Assume that η_i and F_i are measured using the same geometry. Then, for some value of $\pi \leq \pi_t$, $\eta_i(\pi)$ always exhibits a maximum, $\eta_i^{\rm opt}$, and

$$\eta_i(\pi) \leq F_i(\pi) . \tag{A6}$$

If there exists some value P of π such that $F_i(P) > F_i^\infty$, then

$$\eta_i(P) \leq \eta_i^{\rm opt} \leq F_i(P) . \tag{A7}$$

If, however, there is no such value of P, then

$$\eta_i^{\rm opt} \leq F_i^\infty . \tag{A8}$$

If there is no geometry such that P exists, then the relationship (A8) is correct for any geometry, and $\eta_i^{\rm opt}$ should be less than F_i^∞, independent of the geometry used. We believe that this is the case for D^- formation for D^+, D^0, or D^- in a cesium-, rubidium-, or sodium- vapor target, for the energy range considered in the present article.

[1] D. R. Sweetman, A. C. Riviere, H. C. Cole, E. Thompson, D. P. Hammond, J. Hugill, and G. M. McCracken, in *Plasma Physics and Controlled Nuclear Fusion Research* (International Atomic Energy Agency, Vienna, 1971), Vol. III, p. 393–410.

[2] K. H. Berkner, R. V. Pyle, and J. W. Stearns, Nucl. Fusion 15, 249 (1975).

[3] R. Middleton, Nucl. Instrum. Methods 122, 35 (1974).

[4] J. A. Fasolo, IEEE Trans. Nucl. Sci. NS-22, 1665 (1975).

[5] Yu. I. Bel'chenko, G. I. Dimov, and V. G. Dudnikov, Zh. Tekh. Fiz. 45, 68 (1975) [Sov. Phys.—Tech. Phys. 20, 40 (1975)].

[6] K. Prelec and Th. Sluyters, Rev. Sci. Instrum. 44, 1451 (1973); and references therein.

[7] J. Heinemeier and P. Hvelplund, Nucl. Instrum. Methods 148, 65 (1978).

[8] J. John, C. P. Robinson, J. P. Aldridge, W. J. Wallace, K. R. Chapman, and R. H. Davis, Nucl. Instrum. Methods 57, 105 (1967).

[9] B. L. Donnally and G. Thoeming, Phys. Rev. 159, 87 (1967).

[10] A. S. Schlachter, D. H. Loyd, P. J. Bjorkholm, L. W. Anderson, and W. Haeberli, Phys. Rev. 174, 201 (1968).

[11] G. Philip, U. Scheib, and A. Hofmann, Nucl. Instrum. Methods 115, 507 (1974).

[12] D. Hennies, R. S. Raymond, L. W. Anderson, W. Haeberli, and H. F. Glavish, Phys. Rev. Lett. 40, 1234 (1978).

[13] C. W. Drake and R. Krotkov, Phys. Rev. Lett. 16, 848 (1966).

[14] A. S. Schlachter, in *Proceedings of the Symposium on the Production and Neutralization of Negative Hydrogen Ions and Beams*, edited by K. Prelec (Brookhaven National Laboratory, Upton, 1978), pp. 11–23 (BNL Report No. 50727).

[15] H. Bohlen, G. Clausnitzer, and H. Wilsch, Z. Phys. 208, 159 (1968).

[16] W. Grüebler, P. A. Schmelzbach, V. König, and P. Marmier, Phys. Lett. A29, 440 (1969).

[17] W. Grüebler, P. A. Schmelzbach, V. König, and P. Marmier, Helv. Phys. Acta 43, 254 (1970).

[18] A. S. Schlachter, P. J. Bjorkholm, D. H. Loyd, L. W. Anderson, and W. Haeberli, Phys. Rev. 177, 184 (1969).

[19] Yu. M. Khirnyi and L. N. Kochemasova, Prib. Tekh. Eksp. 3, 56 (1970) [Instrum. Exp. Tech. (USSR) 3, 693 (1970)].

[20] F. W. Meyer and L. W. Anderson, Phys. Rev. A 11, 589 (1975).

[21] C. Cisneros, I. Alvarez, C. F. Barnett, and J. A. Ray, Phys. Rev. A 14, 76 (1976).

[22] Y. A. Agafonov, B. A. D'yachkov, and M. A. Pavlii, Pis'ma Zh. Tekh. Fiz. 2, 757 (1976) [Sov. Tech. Phys. Lett. 2, 296 (1976)].

[23] R. J. Girnius, L. W. Anderson, and E. Staab, Nucl. Instrum. Methods 143, 505 (1977).

[24] R. J. Girnius, C. J. Anderson, and L. W. Anderson, Phys. Rev. A 16, 2225 (1977).

[25] A. S. Schlachter, K. R. Stalder, and J. W. Stearns, in *Proceedings of the Tenth International Conference on the Physics of Electronic and Atomic Collisions, Paris, 1977*, edited by G. Watel (Commissariat a l'Energie Atomique, Paris, 1977), Vol. 2, p. 870.

[26] A. S. Schlachter, K. R. Stalder, and J. W. Stearns, in *Proceedings of the XI* ICPEAC, *Kyoto, 1979*, edited by K. Takayanagi and N. Oda (The Society for Atomic Collisional Research, Kyoto, Japan, 1979), pp. 526–527.

[27] T. Nagata, J. Phys. Soc. Jpn. 46, 919 (1979).

[28] T. Nagata (private communication).

[29] F. Meyer, ORNL Report No. 5404, Oak Ridge National Laboratory, 1978 (unpublished).

[30] Y. A. Agafonov, B. A. D'yachkov, and M. A. Pavlii, Sov. Phys.—Tech. Phys. (in press).

[31] B. A. D'yachkov and V. I. Zinenko, At. Energy 24, 18 (1968) [Sov. J. At. Energy 24, 16 (1968)].

[32] B. A. D'yachkov, V. I. Zinenko, and M. A. Pavlii, Zh. Tekh. Fiz. 41, 2353 (1971) [Sov. Phys.—Tech. Phys. 16, 1868 (1972)].

[33] G. I. Dimov and G. V. Roslyakov, Prib. Tekh. Eksp. 3, 31 (1974) [Instrum. Exp. Tech. 17, 658 (1974)].

[34] C. J. Anderson, A. M. Howald, and L. W. Anderson, Nucl. Instrum. Methods 165, 583 (1979).

[35] T. E. Leslie, K. P. Sarver, and L. W. Anderson, Phys. Rev. A 4, 408 (1971). We have renormalized these cross sections upward by a factor of 2.0 to take into account more recent σ_{+0} measurements than those to which they were previously normalized. The absolute

uncertainty of these renormalized cross sections is the previously stated relative uncertainty plus 10% normalization uncertainty, added in quadratures.

[36]R. E. Olson, E. J. Shipsey, and J. C. Browne, Phys. Rev. A 13, 180 (1976). The values for σ_{0-} cited should be divided by four (R. E. Olson, private communication). We consider these results to have been replaced by those in Refs. 40 and 41.

[37]J. R. Hiskes, A. M. Karo, P. A. Willman, and W. J. Stevens, Phys. Lett. 68A, 221 (1978).

[38]R. K. Janev and Z. M. Radulović, Phys. Rev. A 17, 889 (1978).

[39]T. Nagata, in *Proceedings of the XI* ICPEAC, *Kyoto, 1979*, edited by K. Takayanagi and N. Oda (The Society for Atomic Collisional Research, Kyoto, Japan, 1979), pp. 512–513; also, J. Phys. Soc. Jpn. 48, 2068 (1980).

[40]R. E. Olson, Phys. Lett. 77A, 143 (1980).

[41]R. E. Olson and B. Liu, J. Chem. Phys. (in press).

[42]E. R. Salvatelli, G. Lantschner, and W. Mechbach, J. Phys. B 2, 772 (1969); and H. Tawara, At. Data Nucl. Data Tables 22, 491 (1978).

[43]General Ionex model 350 for D^+, D_2^+, and D_3^+; model 358 for D^-.

[44]C. R. Vidal and J. Cooper, J. Appl. Phys. 40, 3370 (1969). We did not use a window or buffer gas as described here.

[45]M. Bacal, A. Truc, H. J. Doucet, H. Lamain, and M. Chretien, Nucl. Instrum. and Methods 114, 407 (1974).

[46]M. Bacal and W. Reichelt, Rev. Sci. Instrum. 45, 769 (1974).

[47]M. Bacal, M. Chretien, H. J. Doucet, H. Lamain, and A. Truc, Ecole Polytechnique Report No. PMI 613, 1973, in French (unpublished).

[48]The target was made by swaging a stainless steel tube over a copper mandrel around which fine stainless steel mesh had been wrapped. The mandrel was etched out in an acid bath and the target fired in vacuum at 600 °C.

[49]Dow Corning 200 oil.

[50]The reservoir was a small cup attached to the center of the target and was sealed with a copper gasket. Two to five grams of cesium, rubidium, or sodium was loaded into the reservoir in a glove box in an argon atmosphere. The reservoir was then momentarily dipped into a liquid-nitrogen bath to lower the temperature (thus reducing the oxidation rate) before being mounted onto the target. A 2-g charge of cesium was sufficient for months of daily running. When cesium or rubidium was loaded into a clean target, the wick was "wet in" by heating the entire target to 180 °C in an argon atmosphere for about an hour; we are not certain that this step was necessary.

[51]R. R. Hultgren, P. D. Desai, D. T. Hawkins, M. Gleiser, K. K. Kelley, and D. D. Wagman, *Selected Values of the Thermodynamic Properties of the Elements* (American Society of Metals, Metals Park, Ohio, 1973).

[52]K. H. Berkner, B. R. Myers, and R. V. Pyle, Rev. Sci. Instrum. 39, 1204 (1968).

[53]M. W. Geis, K. A. Smith, and R. D. Rundel, J. Phys. E 8, 1011 (1975).

[54]We interchangably used materials G1500, HST-41, and G1512 obtained from Gulton Industries, Piezo Products Division, Fullerton, Calif.; their response was similar. We used their model 4D3, referring to 2.54-cm diameter and 1.25-mm thickness. We performed some experiments with Honeywell PLZT composition 1734. The signal was a factor of 3 larger than for the Gulton material; however, the signal-to-noise ratio was the same, which was probably due to microphonics or other external causes.

[55]For a sodium-vapor target, we found that sodium vapor which deposited on the front surface of the detector caused the silver layer to peel off. Instead we used a nickel coating on the pyroelectric ceramic.

[56]The target length for sodium was about 8 cm because a different heater was used.

[57]F. W. Meyer and L. W. Anderson, Phys. Lett. 54A, 333 (1975).

[58]K. H. Berkner, D. Leung, R. V. Pyle, A. S. Schlachter, and J. W. Stearns, Nucl. Instrum. Methods 143, 157 (1977).

[59]K. H. Berkner, D. Leung, R. V. Pyle, A. S. Schlachter, and J. W. Stearns, Phys. Lett. 64A, 217 (1977).

[60]We found that the target plugged with sodium at the very high densities required for equilibrium, perhaps due to inadequately wetting the stainless-steel wick with sodium. We had no such problems with cesium or rubidium.

[61]We do not discuss the results of G. Spiess, A. Valance, and P. Pradel, Phys. Lett. 31A, 434 (1970), because these results are inconsistent with later results by the same group. We also exclude the results of J. H. Kamperschroer and R. S. Post, J. Appl. Phys. 49, 3059 (1978). They obtained large D^- yields in cesium vapor using a Hall accelerator. However, interpretation of the experiment is difficult because of uncertainties in beam intensities. A third paper we do not include is P. Pradel, F. Roussel, A. S. Schlachter, G. Spiess, and A. Valance, Phys. Rev. A 10, 797 (1974). The authors seem to have been unduly critical of their $F_-(\pi)$ result (their Fig. 11 with comment on p. 810). Their target was nearly thick enough for equilibrium, $F_-(\pi)$ appears to be almost flat for their maximum values of π, and their result is in good agreement with the present results.

[62]J. A. Ray, C. F. Barnett, and B. Van Zyl, J. Appl. Phys. 50, 6516 (1979).

[63]D. H. Crandall and J. A. Ray, Rev. Sci. Instrum. 46, 562 (1975); R. H. McKnight, D. H. Crandall, and D. H. Jaecks, Rev. Sci. Instrum. 41, 1282 (1970).

[64]P. M. Stier, C. F. Barnett, and G. E. Evans, Phys. Rev. 96, 973 (1954).

[65]J. B. Taylor and I. Langmuir, Phys. Rev. 44, 423 (1933).

[66]P. Pradel, F. Roussel, and G. Spiess, Rev. Sci. Instrum. 45, 45 (1974).

[67]P. Pradel, F. Roussel, A. S. Schlachter, G. Spiess, and A. Valance, Phys. Rev. A 10, 797 (1974).

[68]A. S. Schlachter, G. Spiess, and P. Pradel, *Proceedings of the Eighth* ICPEAC, *Belgrade, 1973*, edited by B. C. Čobić and M. K. Kurepa (Institute of Physics, Belgrade, 1973), pp. 749–750 determined cross sections from $F_-(\pi)$ yield curves by a fitting procedure. They found that D^- formation was more likely from $D(2s)$ than from $D(1s)$; this unlikely result might have come about because the cross section σ_{-0} was not included in their analysis.

[69]K. H. Berkner, I. Bornstein, R. V. Pyle, and J. W.

Stearns, Phys. Rev. A 6, 278 (1972).
[70]C. S. Lee, D. I. Lee, and C. F. Bonilla, Nucl. Eng. Des. 10, 83 (1969).
[71]M. Makanski, W. A. Selke, and C. F. Bonilla, J. Chem. Eng. Data 5, 446 (1960).
[72]S. K. Allison, Rev. Mod. Phys. 30, 1137 (1958).
[73]The point shown at 10 keV was calculated using the three-charge-component equation for F^{∞}_{-}, because at this energy the effect of the D^{+} fraction is not completely negligible.